

Application of Passive Thermography for Damage Detection in Pavement over Bridge Deck

Ms. Sonia Vasco Da Gama
Civil Engineering Department
Goa College of Engineering
Ponda, India
vascodagamasonia@gmail.com

Dr. Ganesh Hegde
Civil Engineering Department
Goa College of Engineering
Ponda, India
gh@gec.ac.in

ABSTRACT

The Potential reasons for the failure of asphalt overlay on bridge deck is due to poor adhesion between waterproofing membrane and asphalt wearing course, and complex behavior of asphalt layer. By studying the exact behavior of asphaltic layer overlaid on waterproofing membrane under action of dynamic loads and cyclic temperature variation, it is also possible to predict the initiation of debonding and its effect on pavement. In this report behavior of asphaltic layer under the influence of cyclic temperature load has been analyzed. The Finite Element Analysis Technique is used to determine the combined behavior of asphaltic layer and bridge deck. The initiation of debonding and its effect on pavement is studied. Further passive thermography pseudo experiments are conducted on a bridge deck overlaid with asphaltic layer to detect and identify damages in asphalt and base course. The damages were artificially created in the FEM model and passive thermography is simulated. It is found that thermographs obtained clearly shows the presence and extent of damages in the Asphaltic layer. This study helps early detection of debonding and hence enabling repair and replacement strategies at appropriate location without losing much time in locating hidden damages below the road surface which in turn increase the service life of asphalt overlays on concrete bridge decks in Goa.

Keywords—Bridge Deck repairs, service life, Health Monitoring, Waterproofing Membrane, Debonding, Asphaltic layer, Multiphysics Model.

I. INTRODUCTION

This Delamination and rutting of asphaltic layers are commonly observed on the bridge deck which not only affects smooth flow of traffic but also causes further structural distress in the asphaltic layer. These delamination's are mainly due to poor quality of asphaltic layer or sometimes it is also due to poor bonding between asphaltic layer and bridge deck. Extending the usable service life of pavement surface on bridge deck has grown increasingly important in recent years. It is important to have regular inspection to detect initiation of such defects so that corrective repairs are carried out to extend the service life of the pavement layer. Development of early detection technique for assessment of delamination of deck surface has become priority. In this report a simulation is carried out to find effectiveness of using infrared thermography to detect delamination defects in pavement layer on bridge deck. Most NDT for structural elements, such as ultrasonic, magnetic field, and eddy current methods, are suitable for finding flaws between 5 and 100 cm deep, and they have two major drawbacks: they require physical contact with the object being tested, and their scanning-based image generation process is slow. Infrared thermography, sometimes referred to as thermal inspection or infrared imaging, is a quick and distant technique that is increasingly employed in conjunction with other NDT techniques like Ground Penetrating Radar.

In the recent times a new technique is adopted to preserve bridge decks from moisture and temperature deterioration by introducing waterproofing membranes between the deck and asphaltic layer. Although there are many different types of waterproofing membranes, they all work by forming a water-impermeable layer on top of a concrete bridge deck to prevent water and chlorides from infiltrating the deck and causing corrosion of the steel reinforcement and deterioration of the concrete. The most often waterproofing systems are preformed roll-on membranes and liquid applied waterproofing membranes. Generally, preformed and liquid applied membranes are constructed by putting a priming layer to an exposed concrete bridge deck. After that, the

waterproofing membrane is put on top of the priming layer. The membrane is sprayed with a tack layer before being paved over with typical paving asphaltic layer [7].

A variety of factors influence the performance and bond strength of waterproofing membranes with pavement layer. The temperature of the concrete bridge deck during waterproofing membrane installation has been found to have a substantial impact on the binding between the membrane and the deck. Another aspect influencing bond resistance and surfacing effectiveness is bridge deck roughness during construction. Application of primer layer also affects bonding, if the deck becomes too heated, the viscosity of the liquid membrane decreases, resulting in irregular thicknesses and if the deck is too cold, the primer layer will set before it can penetrate [7]. The loss of a bond between the surfacing and the deck prevents the system from functioning as a monolithic structure and diminishes structural integrity. Infrared thermography can be effectively used to determine delamination in asphaltic layer. Infrared thermography is a widely used technique for detecting of damages inside the concrete, railroads and highway bridge decks. Infrared thermography (IRT) can produce images of surface temperature fluctuations linked to subsurface damage at distances of up to 30 metres [8]; it has the capacity to increase inspection efficiency without requiring physical access or traffic control. Additionally, it enables an inspector to quickly scan a vast area to determine which parts of a bridge require repair and which require additional inspection. The main objectives of this study are:

- To model the bridge deck using finite element method to simulate combined physical behaviour of asphaltic layer, waterproofing layer and bridge deck.
- To study the factors affecting debonding of asphaltic layer on the bridge deck
- Find the effect of waterproofing membrane on the behavior of asphaltic layer under different loading conditions
- Using Infrared Thermography principles to identify variations of stresses and damages on a bitumen layer over bridge deck.

II. METHODOLOGY

In this study two types of bridge deck were modelled with identical geometry, Model 1 which has a concrete bridge girder, concrete deck slab and asphalt overlay, while Model 2 has a waterproofing membrane between the concrete deck slab and asphalt overlay. The geometry of models is meshed into finite elements [6]. FEM model is prepared using industry standard software COMSOL. The models were subjected to the heat load to simulate actual site conditions.

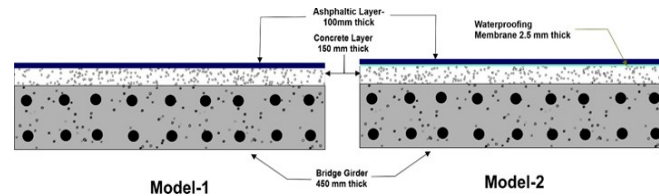


Figure 1: Cross Section of bridge deck with and without waterproofing membrane

A. FE Modelling

In this study to simulate the combined behaviour of asphalt, waterproofing membrane and bridge deck, time dependent heat transfer physics principles are incorporated in COMSOL Software. First, the geometry of the deck slab, waterproofing layer, asphaltic layer is created. The geometry details are as follows: the span of bridge deck is 10m, width 4.25m. The thickness of the girder 450 mm and concrete layer above bridge deck is 150mm. A waterproofing layer of 2.5 mm thickness and asphalt layer of 100mm thickness is provided. The bridge deck is provided with two layers of 20mm diameter bars @ 225mm/c and distribution reinforcement of 12mm bars @200mm/c. The material proprieties as shown in Table1, is assigned to each layer. The geometry is discretized into triangular and tetrahedral elements. The heat flux boundary conditions are assigned and the Heat Transfer module is set up. The heat flow by convection is included as boundary condition acting on all surfaces of bridge deck. The meshing is configured in such a way that adaptive refinement is achieved at boundary of each layer. The total geometry discretized into 11, 50,798 tetrahedral and 2, 60,346 triangular elements as shown in figure 2.

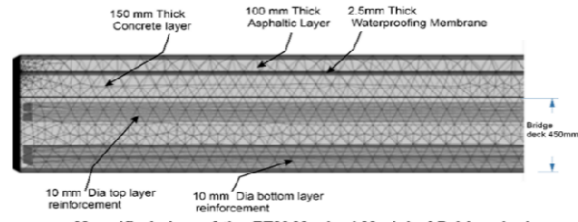


Figure2:FEM model of bridge deck with waterproofing membrane with asphalt layer overlay

Table 1: Material Properties

	Materials			
	Concrete	Steel	Asphalt	Membrane
Thermal Conductivity $k(W/mK)$	1.8	44.5	1.63	0.8
Heat capacity $C_p(J/kgK)$	880	475	1350	1700
Density $\rho(kg/m^3)$	2300	7850	2400	1150
Heat Transfer Coefficient $h(W/m^2K)$	22.138	-	76	-
Youngs Modulus $E(GPa)$	25	200	8	1.4

To simulate identification of damages using infrared thermography, the damages were incorporated in the model as shown the figure 3. The damages are incorporated in asphaltic layer as well as in the concrete base. The defects were of two categories. First one is of defect in the asphaltic layer having loosely damaged asphaltic materials simulating similar to rutting on the road surface. Second type of damage simulated is a completely worn-out asphaltic patches like pot holes and internal cavities inside the asphaltic layer. The Model is subjected to Solar heating and surface temperature profiles are recorded to simulate the infrared thermography.

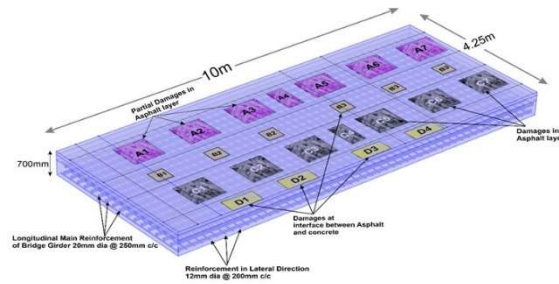


Figure3: Model with Damages

B. FE Analysis

In the first analysis temperature load in the form of flux is applied to both models for 60 minutes and the temperature variation in each layers of both model are recorded. It is observed that in the model 1 the asphaltic layer temperature increased up to 52⁰C while girder temperature reached to 34⁰C steadily. It can be seen that there exists a temperature gradient between asphaltic and girder. In model 2 the temperature of waterproofing layer shown a nonlinear variation compared to temperature variation of asphaltic layer and girder. The temperature variations of different layer of both the models are shown in figure 4. The study reveals that the temperature gradient between various layers is clearly noticeable, and the temperature fluctuation results in unequal expansion under heat loading.

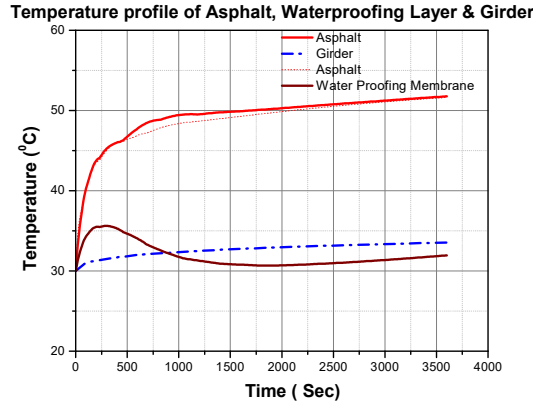


Figure4: Temperature - Time Profile of comparison of maximum temperature on the bridge deck: Model 1v/s Model 2

In the second analysis to simulate the infrared thermography both the models were subjected to Ambient solar heating. The primary source of heat in this analysis is solar irradiation, which is included using the External Radiation Source feature available in COMSOL. This feature uses the longitude, latitude, time zone, day of year, and time of day to compute the direction of the incident solar radiation over the simulation time. The bridge location city Panjim – Goa has been taken with longitude 15.50N Latitude-73.830E, time zone +5.30 UTC, day of the year 17/02/2023, assuming no cloud cover, the solar flux at the surface is about 1000 W/m². The temperature profiles are recorded at different time which shows the presence of damages.

C. Heat Transfer Theory

The analysis to simulate the actual sun heating is carried out as explained above. The numerical model is discretized into finite elements and solar irradiation is applied. The analysis is carried out to simulate natural heating by sun and further cooling. This simulation is carried out for one cycle of 24hrs. The analysis mainly consists of calculating heat produced stress and strains in the finite elements. The analysis considers the natural convection and solar irradiation using following equations. Heat transfer occurs externally by radiation and convection and spreads through material by conduction [1]. Rate of transfer of heat by conduction inside deck is calculated by Fourier law

$$Q_{\text{cond}} = -k\nabla T \quad (1)$$

K is thermal conductivity

∇T is the Temperature gradient in area where rate of transfer of heat by conduction is being studied. Negative sign is due to second law of thermodynamics which says heat always flows in direction of decreasing temperature [6]

Rate of transfer of heat by convection considers interaction between solid and fluid in motion when they are at different temperatures [1] as expressed by Newton's law of cooling given as

$$Q_{\text{conv}} = h(T_s - T_f) \quad (2)$$

h- is the heat transfer coefficient

T_s- is temperature of Surface

T_f- is temperature of fluid (air temperature)

The thermal energy transferred by convection represents a complex mechanism of heat transfer as it depends on the type of fluid flow, fluid properties, and solid surface characteristics, such as geometry and roughness [6]. The solar irradiation heat flux received by external surface of model [1] expressed as

$$Q_{\text{sol}} = \alpha I_{\text{sol}} \quad (3)$$

α absorption coefficient of surface which depends on texture of surface

I_{sol} total solar radiation of surface

The total solar radiation depends on the geographic location of the sample and the Sun orientation (zenith angle and solar elevation), where the latter varies throughout the day and the year [10].

The hourly ambient temperature variation was also used as a boundary condition. The diurnal variation of the ambient temperature (T_{amb}) follows a simple sinusoidal periodic distribution of 24 h, depending on the average daily temperature (T_{avg}) [9]

$$T_{\text{amb}} = T_{\text{avg}} + \Delta T * \cos\left(2\pi \frac{t-14}{24}\right) \quad (4)$$

T_{avg} average daily temperature

ΔT half of the daytime temperature variation

1.1 Thermogram

The analysis of the both the models were carried out as explained above. As the model were discretized in to number of finite elements it is possible to extract thermal contrast between each layer i.e., sub surface temperature contours for both the healthy and target delaminated areas are possible. The thermogram are visual display of the amount of infrared energy emitted, transmitted and reflected by the object. In other words, it can be stated that thermogram is a photograph that shows difference in temperature between different part of an object.

The thermogram for each layer can be extracted from the COMSOL analysis for viewing thermal contours. The thermal results can then be visualised in the COMSOL graphical interface, plotted using 2D plots and exported as Images or data in spreadsheet for further application to damage detection.

To enable surface temperature comparison, the temperature range of the thermograms was unified, and the colour palette was altered to improve the visualisation of the damages in each model. The chosen palette is a unified scale, with yellow representing the greatest surface temperatures and red representing the lowest surface temperatures. The thermograms are extracted from the analysis for time period of 5:00 a.m. to 8:00 a.m. (Morning Session) and 18:00 p.m. to 21:00 p.m. (Evening Session), indicating heating up and cooling down phases as in the actual field condition recorded during the passive IRT inspection. The thermograms extracted for model 1 shown in figure 5 for morning and figure 6 for evening session. Figure 7 and Figure 8 shows the thermograms extracted for Model 2 at morning and evening. Thermograms were extracted for every 2 hours.

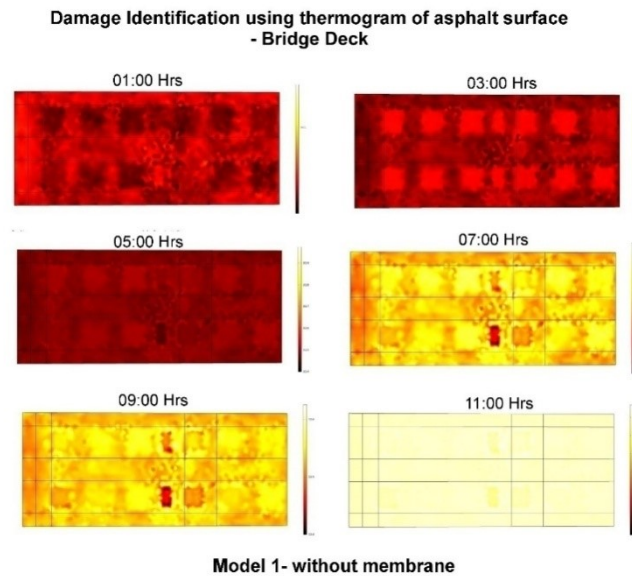


Figure 5: Damage on surface of Model 1 during morning session

D. Damage Identification using Thermograms

The thermal images i.e., thermogram as extracted above clearly show that the simulated damage areas are identified through thermal contrast when the temperature difference between damaged portion and healthy area is greater than $0.5\text{ }^{\circ}\text{C}$. In the above thermograms it can be seen easily that there is temperature contrast i.e., difference between damaged portion and healthy portion of the asphaltic layer. The thermogram are effective in identifying damages even at the subsurface level as shown in figure 5,6,7 and 8.

However, during the interchange time zone of day heating and night cooling, the damaged areas go unrecognizable through the thermal imaging camera i.e., thermograms in this simulation study. It can thus be concluded that the detectability of debonding depends on the thermal conductivity of the material causing it. Thus, the most suitable time to inspect using infrared thermography would be during night-time since debonding would be distinguishable for greater durations. The inspection can be planned accordingly.

From the thermograms it is seen that damages simulated within 100 mm asphaltic layer is seen in both the model. It is seen from figure 5 that the damages which are closer to the surface and having thickness of damage between 10 to 20 mm are clearly seen for longer time.

The damages in concrete layer which are just at the interface between asphaltic layer and concrete are also seen. However, the damages in the concrete layer (below 100 mm) are not seen on the thermogram.

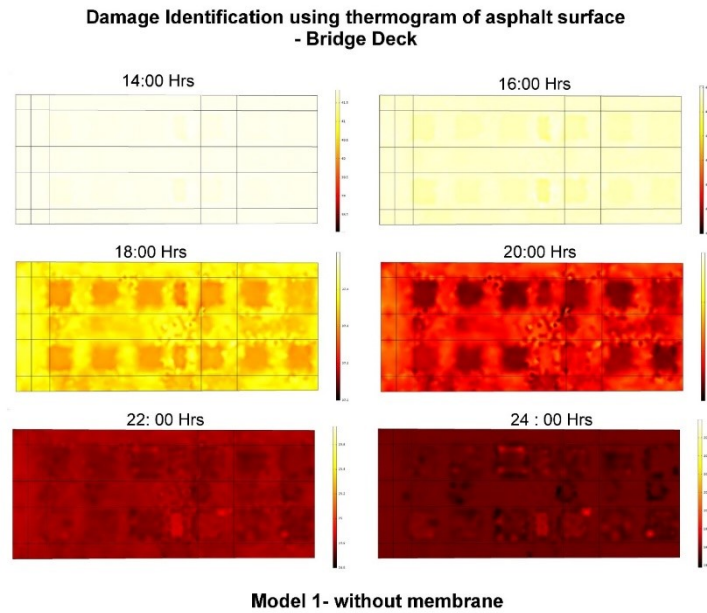


Figure 6: Damage on surface of Model 1 during Evening session

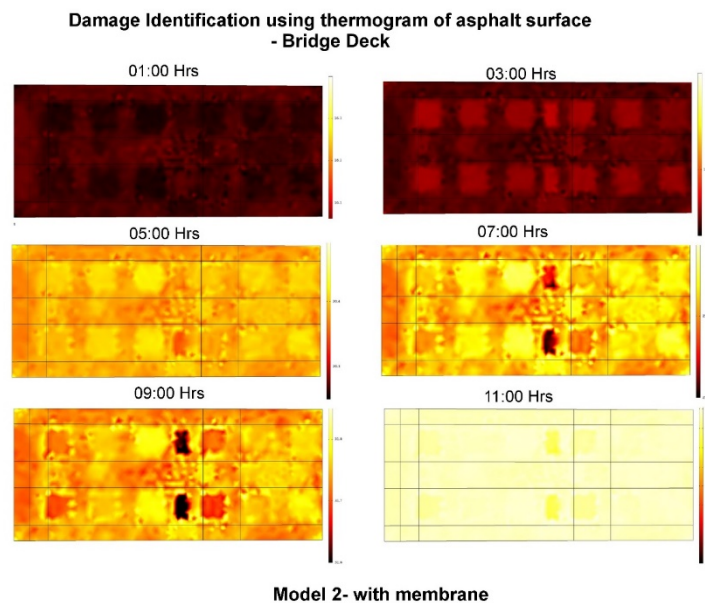


Figure 7: Damage on surface of Model 2 during Morning Session

From this study we can state that damages in the asphaltic layer in model without water proofing membrane is clearly visible at time 3AM to 9 AM in the morning and 6PM to 9PM in the evening. The damages in model 2, with waterproofing membrane, are clearly seen between 3 AM to 9AM in the morning and 5PM to 10 PM. In the evening.

Nearly all the defects of Model 1 and model 2 were visibly identifiable from the thermographs extracted at time periods mentioned above except for B3 and D4 which were modelled and placed in the concrete layer at depths more than 100mm as shown in figure 3.

Defects A4, C4, A5 and C5 were closer to top surface of asphalt having depth of 20 and 10mm respectively retained a distinct thermal contrast for a time periods of even 5hrs after sunrise (1 hrs).

Referring to figure 3, Defects B3, D1, D2 and D3 placed in concrete ie below the 10cm of asphalt layer were not distinctively visible. In model 1 D1 and D3 with property of worn-out asphalt were visible at 9hrs in the

morning while D2 and D4 present in the concrete layer weren't visible in thermograms extracted in Morning as shown in figure 5.

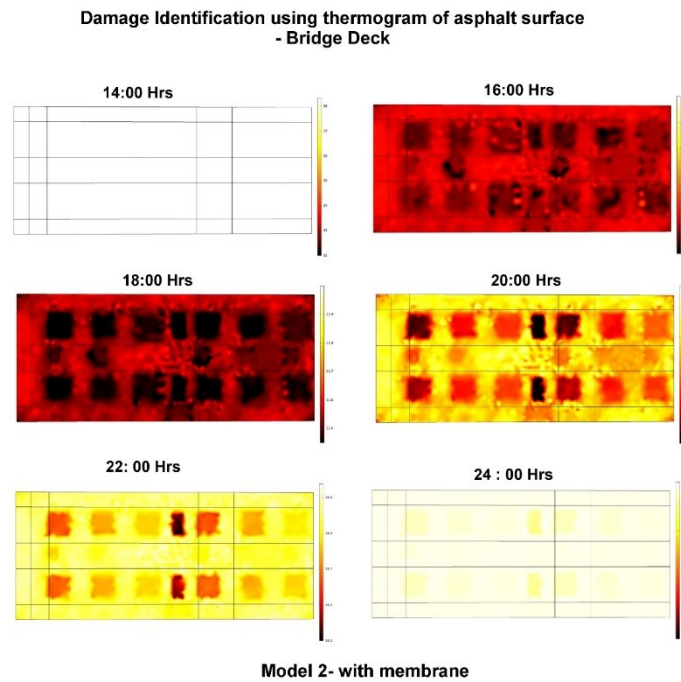


Figure 8: Damage on surface of Model 2 during Evening session

While in the evening at 18 hrs D1, D2 and D3 are clearly visible and D3 at depth of 80mm from top surface continued to be visible from 18hrs to 21hrs as shown in Figure 6.

For Model 2 which is having waterproofing membrane, the defects D1, D2 and D3 were seen in thermographs extracted from 7 hrs to 9 hrs in morning while only D1 and D3 visible from 18hrs to 20 hrs. as shown in figure 7 and figure 8 respectively.

E. Prediction of Delamination of Asphaltic Layer

The prediction of delamination in asphaltic layer is type of reverse engineering with numerical model being updated with the actual thermograms from the IR camera. In this study a numerical model simulated is being used for developing the technique for prediction of delamination. From the numerous multiple analyses conducted on the numerical model we can notice that there is abrupt change in temperature where there are damages.

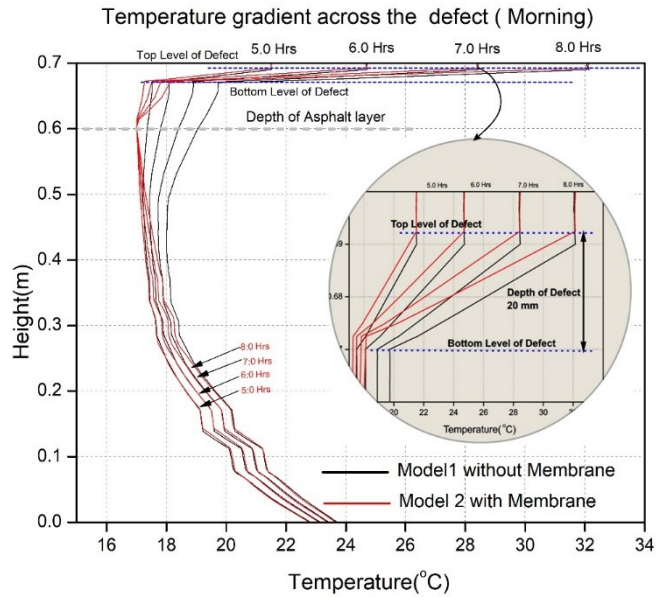


Figure 9: Comparison of worn-out defects in asphaltic Layer for a Temperature profile at various depth of Overlay over Time in Model 1 and Model 2 in Morning Hours

As the main focus of this study is to find actual reason of debonding of asphaltic layer that has occurred on the newly constructed bridge at Panaji Goa, the previous multiple simulation study has revealed unequal expansion and contraction due temperature gradient as the main reason for delamination. Further to justify the previous findings another set of simulations were carried out on the numerical model of bridge deck infused with actual damages. In this simulation the damages were modelled as air voids to replicate the similarity to that of potholes and underneath cavities formed in the asphaltic layer. The analysis results were plotted and thermograms were obtained as shown from figure 5 to figure 8.

Further the temperature gradient obtained across the depth of cross section taken through the damages is shown in figure 9 and figure 10. The damages and the depth of damages is clearly marked by the abrupt change in temperature gradient. The simulation study reveals that the early morning and late evening observation by IR camera will give temperature contrast for clear identification of damages.

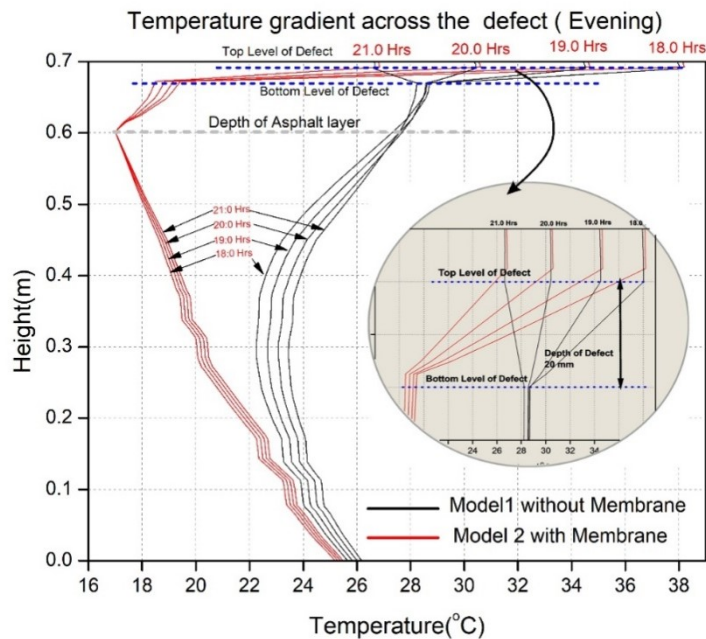


Figure 10: Comparison of worn-out defects in asphaltic Layer for a Temperature profile at various depth of Overlay over Time in Model 1 and Model 2 in Evening Hours

III. RESULTS AND DISCUSSION

Due to the temperature difference, a temperature gradient developed between layers, which resulted in unequal expansions of each layer. The temperature at the top of the asphalt layer and the bottom of the girder is significantly greater than the temperature at the membrane layer, causing a relative displacement between asphaltic and waterproofing membrane that resulted in a relative stress in the asphaltic layer and, ultimately, causes the asphalt to debond. Also, from the graph in figure 4 it is seen that Temperature variations are proportional in Model 1, while model 2 doesn't show proportional variation in temperature between asphaltic layer and waterproofing membrane, this is due to the materials having different coefficient of thermal expansion.

One of the thrusts in this study is to determine whether the damages which are much below the asphaltic layer are identifiable using thermographs. The figure 11 shows the details of damages seen on the thermographs extracted at 18:00 hours on model 1. It is observed that all the damages which are in asphaltic layer (100 mm thick) are visible. However, the damages which are below the asphaltic layer are not clearly visible.

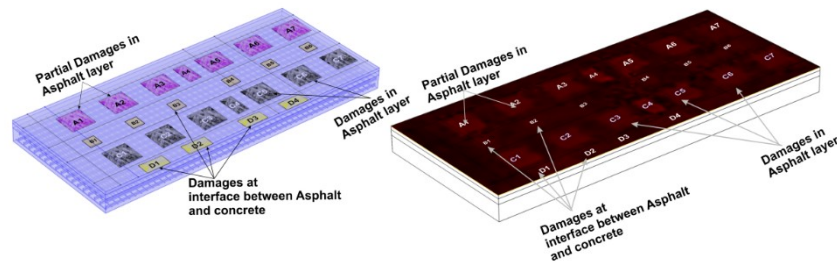


Figure 11: Model 1 Thermal Image extracted at 18:00 Hrs

The damages incorporated in Model 2 are mapped in figure 12 on the thermograph recorded at 21:00 hours. The damages located below the surface up to depth of 100 mm are clearly visible.

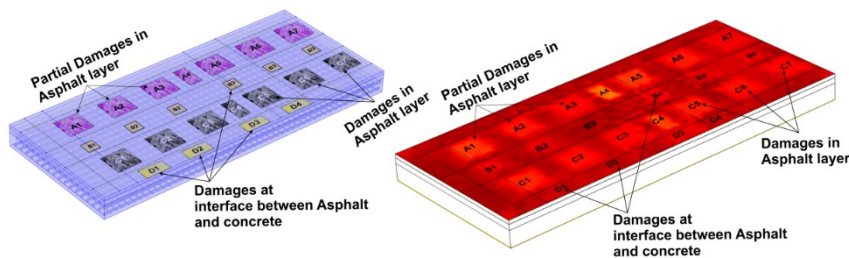


Figure 12: Model 2 Thermal Image extracted at 21:00 Hrs

A correlation exists between amount of solar energy imparted on the surface of bridge deck and amount of thermal contrast observed. Data was analysed to find out the most favourable time of day to carry out inspection when thermal contrast would be greatest, as the depth of defect increases so does development of thermal contrast.

IV. CONCLUSIONS

The bridge deck with asphaltic layer and water proofing layer is studied for its thermal behavior using heat transfer principle. The Finite element analysis is conducted to understand complex behavior of pavement over bridge due to combined effect of waterproofing layer and asphaltic layer. It is found that the relative displacement due to unequal expansion caused to temperature gradient among different layers caused debonding of asphalt on bridge deck. It is concluded that the waterproofing layer between concrete and asphalt is responsible for generating unequal thermal stresses in the pavement layer. It is suggested that waterproofing material which has similar thermal conductivity may be used between asphalt and girder.

The objective of this research is to evaluate the ability of infrared thermography to detect subsurface debonding in asphalt overlay and to estimate a suitable duration for the same. The thermal images show clearly that the thermal imaging camera detects de-bonded areas when their thermal contrast with the bonded area is larger than

0.5 °C. The detectability of debonding is dependent on the thermal conductivity of the material. As a result, the best time to investigate using infrared thermography would be at night, when debonding is visible for longer periods of time. Hence inspection should be scheduled accordingly.

This method of detection has limitations, that it is only effective for superficial subsurface defects in asphalt pavements, up to 100 mm as shown in the extracted thermographs, and it is unable to locate flaws at deeper depths. However, because it can quickly scan large areas, it is highly preferred for field inspections and data collecting as it reduces labor costs and data collection time. It is also harmless for the environment as it only uses thermal radiations and the instrument itself does not emit

REFERENCES

- [1] Pozzer, S.; Dalla Rosa, F.; Pravia, Z.M.C.; Rezazadeh Azar, E.; Maldague, X. Long-Term Numerical Analysis of Subsurface Delamination Detection in Concrete Slabs via Infrared Thermography. *Appl. Sci.* 2021, 11, 4323. <https://doi.org/10.3390/app11104323>
- [2] Haynes, M., Coleri, E., & Obaid, I. A. (2021). Performance of Waterproofing Membranes to Protect Concrete Bridge Decks. *Transportation Research Record*, 2675(9), 1693–1706. <https://doi.org/10.1177/03611981211009527>
- [3] Russell, H. G. (2012). Waterproofing Membranes for Concrete Bridge Decks. *Transportation Research Board*.
- [4] Frosch, R. J., Kreger, M. E., & Strandquist, B. (2013). Implementation of Performance-Based Bridge Deck Protective Systems. <https://doi.org/10.5703/1288284315214>
- [5] Tsubokawa, Y., Mizukami, J., Esaki, T., & Hayano, K. (2007). Study on Infrared Thermographic Inspection of De-bonded Layer of Airport Flexible Pavement. 2007 Worldwide Airport Technology Transfer Conference Federal Aviation Administration American Association of Airport Executives.
- [6] Yçengel, A.; Ghajar, A.J. *Heat and Mass Transfer: Fundamentals & Applications*, 5th ed.; McGraw Hill Education: New York, NY, USA, 2015
- [7] Haynes, M. A., Coleri, E., & Obaid, I. (2021). Performance of waterproofing membranes to protect concrete bridge decks. *Transportation Research Record*, 2675(9), 1693–1706. <https://doi.org/10.1177/03611981211009527>
- [8] Hiasa, S. (2016). Investigation of infrared thermography for subsurface damage detection of concrete structures.
- [9] COMSOL. Parasol and Solar Irradiation. 2019. Available online: <https://www.comsol.com/model/sun-s-radiation-effect-on-tw-coolers-placed-under-a-parasol-12825> (accessed on 10 October 2020).
- [10] Rumbayan, R.; Washer, G.A. Modeling of Environmental Effects on Thermal Detection of Subsurface Damage in Concrete. *Res. Nondestruct. Eval.* 2014, 25, 235–252.